

available at www.sciencedirect.comwww.elsevier.com/locate/brainresBRAIN
RESEARCH

Research Report

Non-invasive electrical stimulation of the brain (ESB) modifies the resting-state network connectivity of the primary motor cortex: A proof of concept fMRI study

G. Alon^{a,*}, S.R. Roys^b, R.P. Gullapalli^b, J.D. Greenspan^c^aUniversity of Maryland, School of Medicine, Department of PTRS, Baltimore, MD, USA^bUniversity of Maryland, School of Medicine, Magnetic Resonance Centre, Baltimore, MD, USA^cUniversity of Maryland Dental School, Department of Neural & Pain Sciences, Baltimore, MD, USA

ARTICLE INFO

Article history:

Accepted 3 June 2011

Keywords:

fMRI

tDCS

tPCS

Resting-state

Brain

Connectivity

ABSTRACT

An innovative method to obtain fMRI resting-state network maps during non-invasive electrical stimulation of the brain (ESB) was developed and tested. Five healthy volunteers participated in 2 fMRI sessions. In session one, a transcranial direct current stimulator (tDCS) was applied placing the positive electrode (31.5 cm²) over the right M1 of the cortex and the negative electrode (31.5 cm²) over the left supra-orbital area of the head. In session two, a monophasic pulsed current stimulator (tPCS) was applied using the identical electrode placement. Imaging was performed on a Siemens 3 T Tim Trio scanner with a 12-channel head coil. At each session, five consecutive functional scans were obtained: 1) resting-state without stimulation (Rest-1), 2) a motor scan consisting of self-paced, bilateral finger–thumb opposition task, 3) resting-state with ESB (Stim-1), 4) resting-state without stimulation (Rest-2), and 5) resting-state with ESB, replicating Stim-1 (Stim-2). Data were analyzed using AFNI and MATLAB. For motor task fMRI analysis, a general linear model (GLM) determined the voxels in the right and left M1 that were significantly correlated with the motor task paradigm. The resting-state time series from the voxels in the R-M1 were averaged and the resulting time series used as a regressor in a GLM analysis to identify M1 connectivity maps. Connectivity maps were quantified as R² values, and then combined to give overlap maps for each of the experimental conditions. Fourier analysis determined the energy in the normalized signal average time courses extracted from L-M1 and R-M1 for each of the resting-state scans. Both tDCS and tPCS lowered the R² values and energy of the averaged time course in the right and left M1 ROI. The effect of the tPCS appeared more pronounced and less variable among subjects. Applying non-invasive ESB during fMRI scanning may down regulate the motor cortex's resting-state network connectivity.

© 2011 Elsevier B.V. All rights reserved.

1. Introduction

Non-invasive electrical stimulation of the brain (ESB) appears to provide simple and minimal risk option to undo some deficits in

neural network communication within the central nervous system (CNS). Using either direct current (tDCS) or pulsed current (tPCS) can alter CNS connectivity (Bolognini et al., 2009; Zaghi et al., 2009). These stimulators have been shown to be very safe

* Corresponding author at: University of Maryland, School of Medicine 100 Penn Street Baltimore, MD 21201 USA. Fax: +1 410 706 6873.
E-mail address: galon@som.umaryland.edu (G. Alon).

when applied to children with cerebral palsy (CP), (Alon et al., 1998) or adults of diverse ages (Bolognini et al., 2009; Celnik et al., 2009; Ferrucci et al., 2009; Gabis et al., 2009; Lefaucheur, 2009; Poreisz et al., 2007; Williams et al., 2009; Wu et al., 2008). Favorable, measurable clinical outcomes are mounting in scientific publications including diagnoses such as Parkinson's Disease (PD), (Boggio et al., 2006; Fregni et al., 2006; Wu et al., 2008) patients with damage to the brain following stroke, (Boggio et al., 2007; Celnik et al., 2009; Hesse et al., 2007; Hummel et al., 2005; Nowak et al., 2009; Schlaug et al., 2008) clinical depression, (Arul-Anandam and Loo, 2009; Ferrucci et al., 2009; Gabis et al., 2009; Nitsche et al., 2009) and chronic pain (Gabis et al., 2009; Mori et al., 2009). The modes of action (mechanisms) leading to the reported clinical results are still in the exploratory phase of research (Polania et al., 2010, 2011).

Several groups of investigators have addressed fundamental electrophysiological questions leading to an apparent consensus that the effects of ESB appear to depend on the direction of the electric current flow. Accordingly, non-invasive ESB alters cortical excitability and activity by enhancing connectivity for brain regions underlying the positive electrode (anodal stimulation) and diminishing excitability for brain regions under the negative electrode (cathodal stimulation) (Schlaug et al., 2008). Positioning the electrodes over the cortical target of stimulation may prove critical (Bolognini et al., 2009; Sadleir et al., 2010) and so the stimulation dosage is typically calculated as the product of stimulation intensity (current amplitude) and treatment time (Reis et al., 2009). From a safety perspective, most investigators prefer to limit the current intensity of tDCS and tPCS to 2 mA (4 mA peak for tPCS) (Alon et al., 1998; Poreisz et al., 2007).

Formulating and affirming the likely mechanism by which ESB promotes enhancement or diminution of CNS excitability has become possible with the advent of non-invasive imaging technologies, most notably magnetic resonance imaging (MRI). Functional magnetic resonance imaging (fMRI) measures of blood oxygenation level-dependent (BOLD) signals can be used to study brain regional resting-state activity (Shehzad et al., 2009). Increased BOLD signal magnitude as a result of activation of local excitatory neurons provides the basis for the interpretation and utilization of fMRI as an objective outcome measure in studying the effects of ESB on CNS connectivity (James et al., 2009).

To date, two polarity-dependent types of stimulators are commercially available in the USA, generically labelled tDCS and tPCS. tDCS delivers a continuous, uninterrupted, non-modulated constant direct current. Direct current is known to alter the electric field, particularly immediately under the electrodes. tPCS delivers the current in a form of unidirectional or bidirectional pulses having very short duration (typically lasting few micro or milliseconds) and various frequencies (typically ranging from few, to several thousand pulses per second). tPCS can alter the electrical field and concurrently excite peripheral nerves located under the electrode (Zaghi et al., 2009). Furthermore, due to the inverse relation between frequency and impedance, opposition to current flow during tPCS application is considerably less than during tDCS application. These fundamental differences suggest that the effects of tDCS and tPCS on CNS connectivity may differ; this hypothesis is tested in this study.

Two recent studies demonstrated the feasibility of using tDCS while obtaining fMRI data (Antal et al., 2011; Kwon et al., 2008). However these studies were limited to assessing the effect of tDCS on the magnitude of the BOLD signal. Here we proposed a novel, proof of concept approach whereby tDCS or tPCS is applied to affect the resting-state connectivity maps during functional magnetic resonance imaging (fMRI). We hypothesized that the resting-state connectivity between the right and left primary motor areas (M1) of healthy subjects will be modified by the application of tDCS and tPCS.

2. Results

Electrical stimulation using tDCS or tPCS during scanning did not produce any additional detectible noise in the MR signal. To test the repeatability of the resting-state network maps, we compared the average R^2 values within L-M1 obtained from the R-M1-seeded resting-state correlation images during REST-1 (first non-stimulated resting-state) between the first and second weeks' scans. Values were similar between the first ($R^2=0.371 \pm 0.17$) and second ($R^2=0.502 \pm 0.13$) weeks using the 7 mm spherical seed. Values were somewhat higher, $R^2=0.442 \pm 0.11$ and $R^2=0.531 \pm 0.17$ in weeks one and two respectively using the 75 voxel cluster masks seed. Statistically there was no difference between weeks using the spherical seed ($Z=-1.753$; $P=0.079$) or cluster seed ($Z=-1.213$; $P=0.225$).

Both tDCS and tPCS altered the resting-state network maps (Fig. 2). Group means and standard errors are presented in Fig. 3. The data were normalized to each subject's initial (REST-1) R^2 values. Overall, the average R^2 values decreased 13.7% and 28.5% under tDCS and tPCS respectively during STIM-2. Whereas there were no statistical differences between tDCS and tPCS data at any time point, STIM-2 using tPCS but not tDCS, reached statistical significance compared to REST-1 ($Z=-2.02$, $p=0.043$). The changes in resting-state network maps followed a similar trend for both stimulation conditions, and for both the spherical and cluster mask seeds, having more consistent responses to

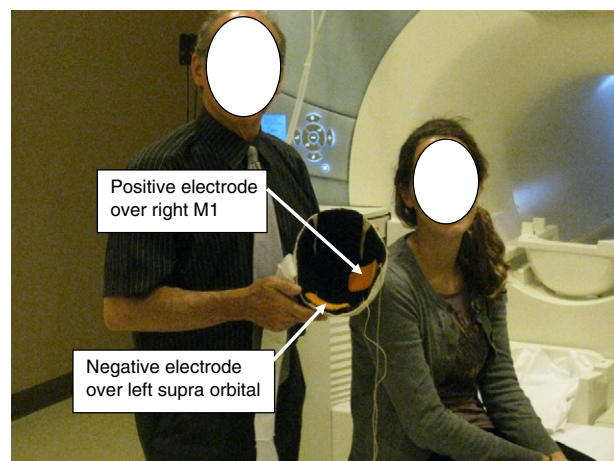


Fig. 1 – Setting up a subject for MRI scanning. The carbon-silicon electrodes were secured within the hermoplastic cup with velcro to assure appropriate positioning throughout the study.

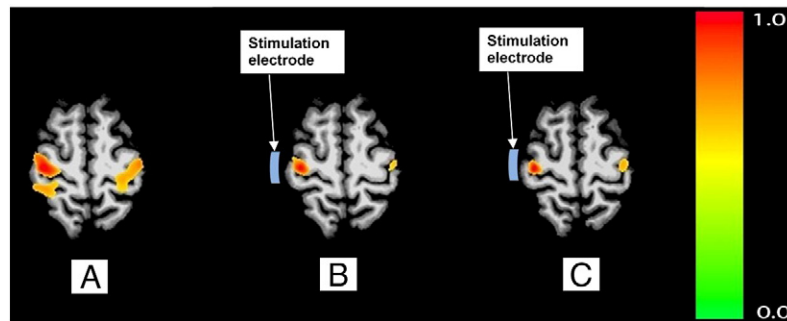


Fig. 2 – Representative motor area resting-state network (MARSN) maps without stimulation (A) with tPCS stimulation (B), and with tDCS stimulation (C) thresholded at $p < 1e-5$. Reduced connectivity between LM and RM areas during either tDCS or tPCS is evident.

tPCS as reflected by the lower coefficient of variation (CoV). Additionally, CoV results showed lower values using the cluster mask seed compared to the spherical seed in seven of eight comparisons (Table 1). Two subjects contributed most to the variability responding to tDCS (Fig. 4) but not to tPCS.

Analysis of the maximum signal amplitude of the power spectral frequency revealed a stimulus-induced change within the right and left motor cortex clusters of interest. Statistical differences in amplitude ($Z = -2.022$; $p = 0.043$) were found comparing the initial non-stimulated REST-1 resting-state (26.8 ± 7.7) with the tPCS STIM-2 resting-state (12.5 ± 3.5). Changes in maximum signal amplitude between REST-1 and STIM-2 during the application of tDCS, while in the same direction, did not reach statistical significance. Fourier analysis of the total energy in the normalized signal clearly indicated less energy during both tDCS and tPCS compared to REST-1 (Fig. 5). Notably, that change persisted after the first stimulation during REST-2.

Subject's perception of the stimuli was distinctly different between tDCS and tPCS. During tDCS all 5 volunteers reported a very mild sensation of tingling and/or itching. During tPCS a

perception of tingling but not itching was accompanied with visualization of repeated flashing light.

3. Discussion

A rapid accumulation of studies including double-blind placebo controlled clinical trials contribute to an expanding consensus that non-invasive ESB promotes further clinical gains among patients with damage to the brain due to trauma, vascular infarct, or neurodegenerative process (Alon et al., 1998; Ben Taib and Manto, 2009; Benninger et al., 2010; Boggio et al., 2007; Fregni et al., 2006; Hummel et al., 2005; Lindenberg et al., 2010; Monti et al., 2008). Attempts to explain the mechanisms that govern the application of ESB include simulation of current flow patterns and current densities around and within the brain (Sadleir et al., 2010) or apply graph theory to map nodal connectivity and minimum path length (Polania et al., 2010, 2011). Both models predict that some of the externally applied current penetrates the skull through various pathways, and hence may directly modify the neural excitability and network connectivity within the brain. Our in vivo human fMRI data clearly indicate that primary measurable changes occurred in R-M1 brain tissue directly under the stimulating electrode.

Several fundamental questions were tested in this proof of concept fMRI study. The primary questions were mostly methodological and included reproducibility of resting-state network maps and the ability to obtain noise-free fMRI data during the application of non-invasive ESB. Being among the first to study

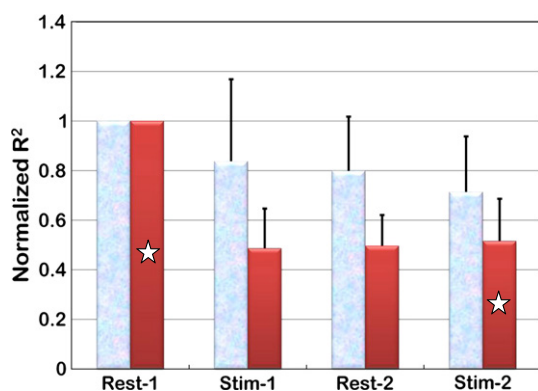


Fig. 3 – Group mean average R^2 values normalized to each subject average R^2 during the non-stimulated resting-state (Rest-1). The light bars represent tDCS and the dark tPCS. Note: There were no statistical differences between tDCS and tPCS data at any time point, however, Stim-2 using tPCS but not tDCS, reached statistical significance compared to its REST-1 data.

Table 1 – Summary of the coefficient of variation (CoV) among subjects using the spherical and cluster mask seeds to identify the most active contiguous voxels.

	tDCS		tPCS	
	Spherical	Cluster	Spherical	Cluster
REST-1	0.26	0.18	0.14	0.11
STIM-1	0.32	0.20	0.14	0.14
REST-2	0.38	0.27	0.28	0.24
STIM-2	0.25	0.21	0.21	0.19
Mean	0.30	0.21	0.19	0.17

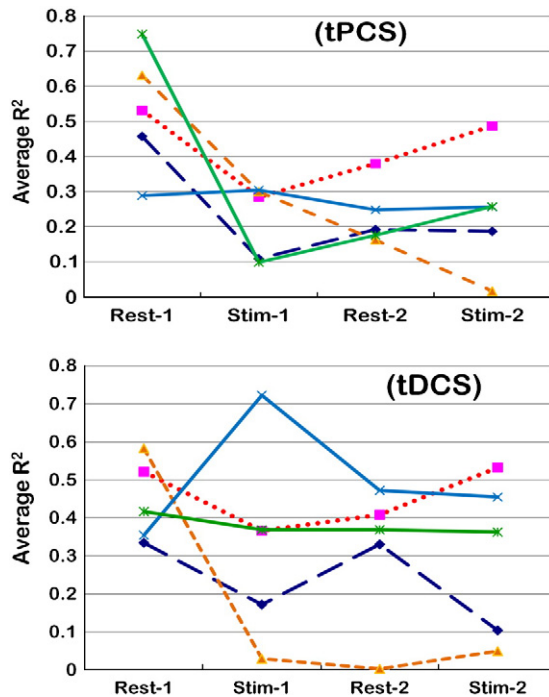


Fig. 4 – Non-normalized average L-M1-R-M1 R^2 values illustrate considerable individual variation during both non-stimulated and stimulated resting-state mapping of the MRI session.

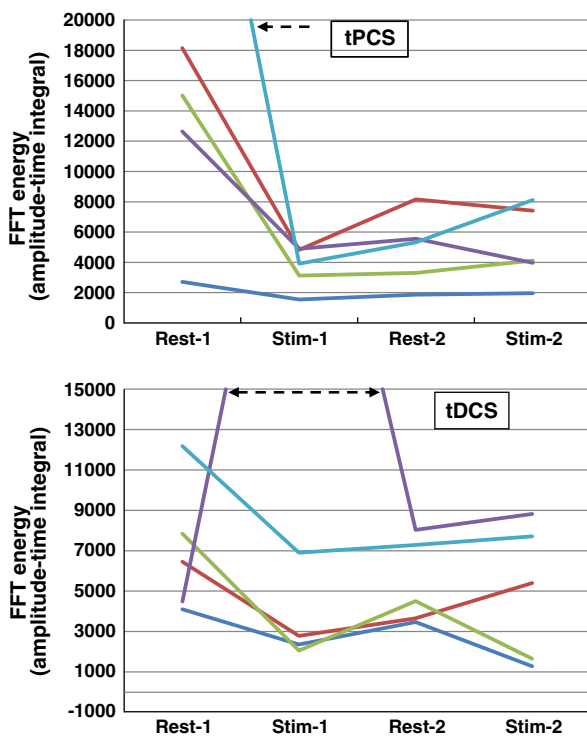


Fig. 5 – Individual variations of the BOLD signals time-amplitude integral (energy) during either tDCS or tPCS stimulation. The dashed arrow indicates cut-off on the graph due to very high signal energy for one subject during tDCS and another during tPCS.

the effect of ESB on the resting-state network maps of healthy subjects, and aware of the considerable inter- and intra-subject variability of fMRI data, we addressed two questions: First, which of two seed ROI options, the spherical boundary or the cluster masks, yield less variable connectivity data? The rationale to compare the common approach of spherical boundary (James et al., 2009) with cluster masks emerged from the observation that hemodynamically active voxels are rarely symmetrical in configuration making it difficult to standardize the ROI. In the current investigation the computer algorithm generated cluster masks containing the 75 most active voxels centered on R-M1 and L-M1 from each scan thus more faithfully representing each individual subject's ROI. The data reported in Table 1 suggest that the cluster mask approach can help reduce the variability inherent in group analysis of fMRI data.

A second methodological question was the repeatability of the resting-state network maps between the left and right primary motor areas. Statistically there was no significant difference between two data sets obtained one week apart supporting acceptable reproducibility (Meindl et al., 2009). However, the high inter-subject variability and only moderate between sessions (intra-subject) correlation ($r=0.57$) supports testing a larger sample size to confirm the findings.

The primary neurophysiological question was whether tDCS and tPCS have similar or different effects on the right-to-left primary motor areas' (M1) resting-state network. The unexpected high variability during tDCS application precludes definitive comparison of tPCS and tDCS effects on the studied network. Qualitatively similar reduction of the resting-state network map occurred during the second set (STIM-2) application of anodal (positive electrode) stimulation placed over the right M1 area, irrespective of the type of stimulator (tDCS or tPCS). The overall decrease in temporal correlation (R^2 values) and Fourier transformed peak amplitude and energy of the signals were not expected because the vast majority of clinical studies support the principle that anodal stimulation enhances cortical excitability. Increased excitability assessed by transcranial magnetic stimulating (TMS) or inferred from improved motor-behavioural performance have been reported by numerous investigators (Arul-Anandam and Loo, 2009; Boggio et al., 2006; Celnik et al., 2009; Floel et al., 2008; Gandiga et al., 2006; Nitsche et al., 2009; Wu et al., 2008).

Our finding of diminished fMRI signal amplitude and energy may complement the most recent report that the BOLD signal in the supplementary motor cortex (SMA) but not the primary motor cortex (M1) diminished during the application of tDCS combined with finger tapping motor task (Antal et al., 2011). Common to both investigations is the application of anodal stimulation over the primary motor cortex during fMRI of healthy subjects. However, there are noteworthy differences in the experimental protocol and data processing between the studies. Antal and colleagues quantified the BOLD signal, counting all active voxels in each of several brain ROI during volitional movements of finger tapping. The tDCS was applied in a block design of 20 s on and 20 s off cycle repeated 8 times. In contrast, we processed the BOLD signals as cluster masks of the 75 most active voxels in the right and left M1 and quantified the resting-state map by the average regressor R^2 between the two primary motor areas' ROI. Moreover, we administered either tDCS or tPCS continuously for 6 min and 24 s and repeated

the stimulation after 6 min and 24 s of non-stimulated resting-state. Antal's group observed a decrease in the number of active voxels in the SMA whereas we recorded significant reduction in resting-state connectivity between the left and right M1. Whether both studies address the same or different mechanism of modifying motor connectivity within the brain requires further study.

It is plausible to propose one or more tentative explanations to the findings that motor-behavioural performance improved following non-invasive ESB. Conceivably, anodal stimulation over the right M1 decreases the resting-state in-phase oscillation of BOLD signals between the right and left M1 (Zuo et al., 2009). The decrease may modify the left-on-right inter-hemispheric inhibition, improve the efferent signal-to-noise ratio over the stimulated side, and lead to a more efficient synaptic transmission resulting in faster motor execution of the extremity movements. Such inhibition was demonstrated in an elegant study of inter-hemispheric interactions during unilateral and bilateral hand movements of healthy subjects (Grefkes et al., 2008). Alternatively, it is possible that during stimulation the BOLD signals are attenuated and the enhanced excitatory response reported clinically, represents a rebound hemodynamic response after termination of the ESB. It is worth noting that typical stimulation time in clinical trials is 20 min whereas our stimulation protocol lasted only close to 13 min, raising the possibility that longer stimulation may be necessary to promote improvement of task performance.

Another tentative explanation can be formulated based on the model of Sadleir's group. The authors presented the most realistic head-brain model to date placing two 22 cm² electrodes, one over F3 (left posterior inferior frontal region), and one over the right supra-orbital region. Whereas current densities were high under both electrodes, other areas not covered by the electrodes exhibit similar magnitudes of current density (Sadleir et al., 2010). It is conceivable that tDCS and tPCS modify the brain's electrical field thereby shifting connectivity of the resting-state network map to areas adjacent to the stimulating electrodes including supplementary motor area (SMA) and pre motor area (PMC). Re-directing the neural network connectivity may provide a means by which non-invasive electrical brain stimulation enhances network communication. This tentative hypothesis requires systematic testing using different experimental protocol than the one used in the current study.

As a group, the effect of tDCS and tPCS on the M1 maps appears similar but the response was less variable using the tPCS. Electrode-skin interface impedance may have been a contributing factor derived from the known association between stimulus frequency and impedance. We estimated impedance by calculating peak voltage to peak current ratios. The group mean was 6789 Ω during tDCS and 4229 Ω during tPCS. Attempts to maintain hydration of the electrodes and hair as well as contact pressure of the electrodes throughout the study imply that owing to lower impedance, transcranial pulsed current may prove advantages over direct current for non-invasive ESB. However, more data must be collected to support or refute this supposition.

The mode of action of tDCS and tPCS may also differ. The tPCS delivered unidirectional pulses so that polarity was the same as the tDCS. Zaghi and co-investigators summarized the known effects of tDCS and bidirectional transcranial stimula-

tor they termed cranial AC. They surmised that direct current modulates spontaneous neuronal activity in a polarity-dependent fashion with site-specific effects and that cranial AC stimulation may not polarize brain tissue, but rather synchronize and enhance the efficacy of endogenous neurophysiologic activity. The authors suggested further, that secondary non-specific central, peripheral or both effects may explain the clinical outcomes of tDCS or cranial AC stimulation (Zaghi et al., 2009). Whether unidirectional pulses as used in our study affect the brain similar to tDCS or cranial AC remains unknown. The typical perception of tingling/itching under the electrodes during tDCS was reported by all five subjects a duplicate of the perception reported by others (Antal et al., 2011). The perception during the tPCS was distinctly different with all subjects reporting tingling and visualization of repeated flashing light but not itching. Taken together, the data obtained in our study suggest that the effects of tDCS and tPCS on the brain are similar. Confirmation or rejection of the proposition that tPCS modifies the fMRI-derived resting-state network maps or affects brain function differently than tDCS will require further investigation.

There are several shortcomings inherent in this proof of concept study. Having only 5 subjects precludes extrapolation of the finding to other healthy volunteers. Second, the resting-state network was limited to two ROI — right and left M1. Expanding the network to include additional ROI critical to motor control such as cerebellum and SMA and adding a performance of a motor task as independent variable should be included in future studies. Such addition may help delineate common and differential effects of tDCS and tPCS on the resting as well as active state network. A null hypothesis that both types of ESB have similar effect on human brain connectivity, and on motor performance of the upper and lower extremities, should be tested in future investigation. Another potential shortcoming was applying continuous stimulation. Antal (Antal et al., 2011) also applied the stimulation over the M1 area, but rather than continuous stimulation, applied the tDCS in a block design of 20 s on and 20 s off cycle repeated 8 times. Continuous vs. cyclic stimulation may have different effect on the BOLD signals, a hypothesis that requires further testing. Finally, the presented protocol was limited to one session of ESB. Whether repeated sessions of non-invasive ESB have longer lasting effects on the* resting and active state network, remains unknown.

4. Conclusion

Non-invasive conductive electric current stimulation of the brain (ESB) either direct or pulsed can be safely applied within a 3 T magnet without any signal degradation. Further, results indicate that (a) ESB is likely to down regulate the resting-state networks map of the primary motor cortex (M1), (b) stimulation effects are persistent for at least 13 min post-stimulation, and (c) the magnitude of the resting-state modification may, or may not be dependent on the type of electrical stimulation provided (tDCS or tPCS). We are unaware of in vivo, human studies reporting direct real-time effects of non-invasive ESB on the brain's resting-state, and our preliminary results suggest that connectivity MRI studies can help refine the methodology of and elucidate more specific mechanisms responsible for therapeutic benefits of ESB.

5. Experimental procedures

5.1. Subjects

Four healthy females and one male, ranging in age between 23 and 27 years, met inclusion criteria including: eligibility check list for MRI, proof of not being pregnant, and freedom from known musculo-skeletal, neurological, or vascular impairments. All aspects of this research protocol were approved by the University of Maryland, Baltimore, institutional review board.

5.2. Description of ESB apparatus

Subjects participated in two MRI sessions separated by one week. In each session, a thin thermoplastic moulded cap that included two 7 cm×4.5 cm (area 31.5 cm²) carbon-silicon flexible electrodes was secured over each subject's head. The positive electrode was positioned over the right primary motor area of the cortex (M1) and the negative electrode over the supra-orbital area on the left side of the head (Fig. 1). The electrodes and hair over M1 were profusely hydrated with water to assure good conductivity. Shielded conductive leads extended from the electrodes to the penetration panel on the side-wall of the magnet room and custom-connected using radio frequency filters to the stimulator in the MRI control room. Two types of battery powered non-invasive ESB stimulators were used in the study. One was a direct current stimulator (tDCS) (Dupel system™, EMPI, St. Paul, MN) that delivered a constant current at 2 mA amplitude (Table 2). The second was a pulsed current stimulator (tPCS) (Fisher Wallace model FW 100-C™, New York, NY) which delivered a monophasic (unidirectional) waveform with a pulse duration of 33.3 μs and an inter-pulse interval of 33.3 μs. The stimulator's carrier frequency was 15 kHz. However, having 1 ms inter-burst intervals, decreased the number of pulses per second to 7500 pulses. These pulses were ON for 50 ms yielding 375 pulses/50 ms. Furthermore, in 1 s there were 15 bursts of pulses, yielding an effective frequency of 5625 pulses per second (15×375). Peak current amplitude was set at maximum output and the actual peak voltage and peak current delivered to each subjects are summarized in Table 2.

5.2.1. MRI

All imaging was performed using a Siemens 3 T Tim Trio scanner with a 12-channel head coil. After obtaining the

appropriate localizer images, a high resolution T1-weighted three-dimensional magnetization-prepared rapid acquisition with gradient echo (3D-MPRAGE) image (TE=3.44 ms, TR=2 s, TI=900 ms, flip angle=9°, 72 slices, slice thickness 2 mm, 0.898×0.898 mm² in-plane resolution and a FOV of 23 cm) was acquired for anatomic reference. Following the acquisition of anatomical data, five separate functional scans were obtained from each subject. The first scan consisted of a resting-state condition without electrical stimulation (REST-1). The second scan consisted of a motor paradigm that involved a self-paced bilateral finger-thumb opposition task using a block design with 24 s On and 24 s Off for a total of 8 cycles. Subjects received signals indicating when to perform the motor task by using a mirror mounted on top of the head coil to view a rear projection computer screen placed at the end of the magnet bore. The third scan consisted of a resting-state condition with continuous tDCS applied (STIM-1). The fourth scan consisted of a resting-state condition with no electrical stimulation (REST-2), followed by the final scan which consisted of a resting-state condition with continuous tDCS applied again (STIM-2). All the aforementioned functional images (including the motor paradigm) were acquired using single-shot twice refocused spin-echo EPI T2*-sensitive sequence (TE=30 ms, TR=3 s, 1.8×1.8 mm² in-plane resolution and a FOV of 23 cm) using 36 axial slices (4 mm thick) with no gap between slices for a total acquisition time of 6 min and 24 s. Overall, the subjects were in the scanner for about 45 min during each visit.

During the first visit the subjects received only tDCS. The exact procedures were repeated with tPCS applied during the subjects' second visit one week later. During ESB, the voltage and current intensities were monitored by a two channel digital storage oscilloscope (Tektronix™ TDS 1002). The total time of stimulation during the tDCS and tPCS session was 12 min 48 s (half during STIM-1 and the other half during STIM-2). For the resting-state scans, subjects were instructed to close their eyes and stay awake.

5.3. Data analysis

Data were analyzed using AFNI (Robert Cox, NIH) and MATLAB (MathWorks Inc., Natick, MA). Images were corrected for slice timing, registered, blurred with a 6 mm full width half maximum (FWHM) Gaussian blur, and intensity normalized. The motor task scans from both visits were concatenated and processed to create a single motor activation image for each subject. The coordinates of the most highly active areas centered on the right primary motor hand area (R-M1) and left primary motor hand area (L-M1) were determined from the motor activation image. By automatically thresholding the motor activation images and analyzing the resulting binary cluster images, two functional cluster masks were created for each subject, each containing the 75 most active contiguous voxels in the subject's motor activation image and containing the coordinates of maximal R-M1 and L-M1 activation respectively. In addition to the functional cluster masks, two 7 mm diameter spherical ROIs were also created for each subject centered on the coordinates of maximal R-M1 and L-M1 activation voxels.

The average time courses from within the R-M1 and L-M1 functional cluster masks were extracted from each of the resting-state scans. The average time courses extracted from the R-M1 cluster were used as regressors on their respective

Table 2 – Peak voltage and peak current measurement during stimulation.

Subject	Peak volt (volts)		Peak current (milliamp) [‡]		Volt/current ratio	
	tDCS	tPCS	tDCS	tPCS	tDCS	tPCS
1.	15.0	16.5	2	3.8	7500	4342
2.	14.8	17.6	2	4.0	7400	4400
3.	19.2	14.4	2	3.8	9600	3789
4.	17.2	17.6	2	2.4	8600	7333
5.	16.6	18.0	2	3.2	8300	5625

[‡] Note: The group mean current density was 0.063 and 0.020 mA per cm² during tDCS and tPCS respectively.

resting-state scans to calculate R-M1-seeded correlation images. From these correlation images, the average R^2 correlation coefficients within the L-M1 cluster masks were computed to determine the degree of correlation between L-M1 and R-M1 during the resting-state scans. The average time courses extracted from L-M1 and R-M1 cluster masks for each of the resting-state scans were also subjected to Fourier analysis to determine the energy in the normalized signal and the maximum amplitude of the dominant frequency component.

Given the small sample size, data analysis was performed using non-parametric Wilcoxon tests ($\alpha=0.05$). The effect of tDCS and tPCS on the primary motor (M1) resting-state network was of particular interest.

REFERENCES

- Alon, G., Syron, S.C., Smith, G.V., 1998. Is transcranial electrical stimulation (TCES) a safe intervention for children with cerebral palsy? *J. Neuro. Rehabil.* 12, 65–72.
- Antal, A., Polania, R., Schmidt-Samoa, C., Dechent, P., Paulus, W., 2011. Transcranial direct current stimulation over the primary motor cortex during fMRI. *NeuroImage* doi:10.1016/j.neuroimage.2010.11.085.
- Arul-Anandam, A.P., Loo, C., 2009. Transcranial direct current stimulation: a new tool for the treatment of depression? *J. Affect. Disord.* 117, 137–145.
- Ben Taib, N.O., Manto, M., 2009. Trains of transcranial direct current stimulation antagonize motor cortex hypoexcitability induced by acute hemicerebellectomy. *J. Neurosurg.* 111, 796–806.
- Benninger, D.H., Lomarev, M., Lopez, G., Wassermann, E.M., Li, X., Considine, E., Hallett, M., 2010. Transcranial direct current stimulation for the treatment of Parkinson's disease. *J. Neurol. Neurosurg. Psychiatry* 81, 1105–1111.
- Boggio, P.S., Ferrucci, R., Rigonatti, S.P., Covre, P., Nitsche, M., Pascual-Leone, A., Fregni, F., 2006. Effects of transcranial direct current stimulation on working memory in patients with Parkinson's disease. *J. Neurol. Sci.* 249, 31–38.
- Boggio, P.S., Nunes, A., Rigonatti, S.P., Nitsche, M.A., Pascual-Leone, A., Fregni, F., 2007. Repeated sessions of noninvasive brain DC stimulation is associated with motor function improvement in stroke patients. *Restor. Neurol. Neurosci.* 25, 123–129.
- Bolognini, N., Pascual-Leone, A., Fregni, F., 2009. Using non-invasive brain stimulation to augment motor training-induced plasticity. *J. Neuroeng. Rehabil.* 6, 8.
- Celnik, P., Paik, N.J., Vandermeeren, Y., Dimyan, M., Cohen, L.G., 2009. Effects of combined peripheral nerve stimulation and brain polarization on performance of a motor sequence task after chronic stroke. *Stroke* 40, 1764–1771.
- Ferrucci, R., Bortolomasi, M., Vergari, M., Tadini, L., Salvoro, B., Giacomuzzi, M., Barbieri, S., Priori, A., 2009. Transcranial direct current stimulation in severe, drug-resistant major depression. *J. Affect. Disord.* 118, 215–219.
- Floel, A., Rosser, N., Michka, O., Knecht, S., Breitenstein, C., 2008. Noninvasive brain stimulation improves language learning. *J. Cogn. Neurosci.* 20, 1415–1422.
- Fregni, F., Boggio, P.S., Santos, M.C., Lima, M., Vieira, A.L., Rigonatti, S.P., Silva, M.T., Barbosa, E.R., Nitsche, M.A., Pascual-Leone, A., 2006. Noninvasive cortical stimulation with transcranial direct current stimulation in Parkinson's disease. *Mov. Disord.* 21, 1693–1702.
- Gabis, L., Shklar, B., Baruch, Y.K., Raz, R., Gabis, E., Geva, D., 2009. Pain reduction using transcranial electrostimulation: a double blind "active placebo" controlled trial. *J. Rehabil. Med.* 41, 256–261.
- Gandiga, P.C., Hummel, F.C., Cohen, L.G., 2006. Transcranial DC stimulation (tDCS): a tool for double-blind sham-controlled clinical studies in brain stimulation. *Clin. Neurophysiol.* 117, 845–850.
- Grefkes, C., Eickhoff, S.B., Nowak, D.A., Dafotakis, M., Fink, G.R., 2008. Dynamic intra- and interhemispheric interactions during unilateral and bilateral hand movements assessed with fMRI and DCM. *NeuroImage* 41, 1382–1394.
- Hesse, S., Werner, C., Schonhardt, E.M., Bardeleben, A., Jenrich, W., Kirker, S.G., 2007. Combined transcranial direct current stimulation and robot-assisted arm training in subacute stroke patients: a pilot study. *Restor. Neurol. Neurosci.* 25, 9–15.
- Hummel, F., Celnik, P., Giroux, P., Floel, A., Wu, W.H., Gerloff, C., Cohen, L.G., 2005. Effects of non-invasive cortical stimulation on skilled motor function in chronic stroke. *Brain* 128, 490–499.
- James, G.A., Lu, Z.L., VanMeter, J.W., Sathian, K., Hu, X.P., Butler, A.J., 2009. Changes in resting state effective connectivity in the motor network following rehabilitation of upper extremity poststroke paresis. *Top Stroke Rehabil.* 16, 270–281.
- Kwon, Y.H., Ko, M.H., Ahn, S.H., Kim, Y.H., Song, J.C., Lee, C.H., Chang, M.C., Jang, S.H., 2008. Primary motor cortex activation by transcranial direct current stimulation in the human brain. *Neurosci. Lett.* 435, 56–59.
- Lefaucheur, J.P., 2009. Methods of therapeutic cortical stimulation. *Neurophysiol. Clin.* 39, 1–14.
- Lindenberg, R., Renga, V., Zhu, L.L., Nair, D., Schlaug, G., 2008. Bihemispheric brain stimulation facilitates motor recovery in chronic stroke patients. *Neurology* 71, 2176–2184.
- Meindl, T., Teipel, S., Elmouden, R., Mueller, S., Koch, W., Dietrich, O., Coates, U., Reiser, M., Glaser, C., 2009. Test-retest reproducibility of the default-mode network in healthy individuals. *Hum. Brain Mapp.* 31, 237–246.
- Monti, A., Cogiamanian, F., Marceglia, S., Ferrucci, R., Mameli, F., Mrakic-Sposta, S., Vergari, M., Zago, S., Priori, A., 2008. Improved naming after transcranial direct current stimulation in aphasia. *J. Neurol. Neurosurg. Psychiatry* 79, 451–453.
- Mori, F., Codeca, C., Kusayanagi, H., Monteleone, F., Buttari, F., Fiore, S., Bernardi, G., Koch, G., Centonze, D., 2009. Effects of anodal transcranial direct current stimulation on chronic neuropathic pain in patients with multiple sclerosis. *J. Pain* 11, 436–442.
- Nitsche, M.A., Boggio, P.S., Fregni, F., Pascual-Leone, A., 2009. Treatment of depression with transcranial direct current stimulation (tDCS): a review. *Exp. Neurol.* 219, 14–19.
- Nowak, D.A., Grefkes, C., Ameli, M., Fink, G.R., 2009. Interhemispheric competition after stroke: brain stimulation to enhance recovery of function of the affected hand. *Neurorehabil. Neural Repair* 23, 641–656.
- Polania, R., Paulus, W., Antal, A., Nitsche, M.A., 2010. Introducing graph theory to track for neuroplastic alterations in the resting human brain: a transcranial direct current stimulation study. *NeuroImage* doi:10.1016/j.neuroimage.2010.09.085.
- Polania, R., Nitsche, M.A., Paulus, W., 2011. Modulating functional connectivity patterns and topological functional organization of the human brain with transcranial direct current stimulation. *Hum. Brain Mapp.* 32 doi:10.1002/hbm.21104.
- Poreisz, C., Boros, K., Antal, A., Paulus, W., 2007. Safety aspects of transcranial direct current stimulation concerning healthy subjects and patients. *Brain Res. Bull.* 72, 208–214.
- Reis, J., Schambra, H.M., Cohen, L.G., Buch, E.R., Fritsch, B., Zarahn, E., Celnik, P.A., Krakauer, J.W., 2009. Noninvasive cortical stimulation enhances motor skill acquisition over multiple days through an effect on consolidation. *Proc. Natl. Acad. Sci. U S A* 106, 1590–1595.
- Sadleir, R.J., Vannorsdall, T.D., Schretlen, D.J., Gordon, B., 2010. Transcranial direct current stimulation (tDCS) in a realistic head model. *NeuroImage* 51, 1310–1318.
- Schlaug, G., Renga, V., Nair, D., 2008. Transcranial direct current stimulation in stroke recovery. *Arch. Neurol.* 65, 1571–1576.
- Shehzad, Z., Kelly, A.M., Reiss, P.T., Gee, D.G., Gotimer, K., Uddin, L.Q., Lee, S.H., Margulies, D.S., Roy, A.K., Biswal, B.B., Petkova, E.,

- Castellanos, F.X., Milham, M.P., 2009. The resting brain: unconstrained yet reliable. *Cereb. Cortex* 19, 2209–2229.
- Williams, J.A., Imamura, M., Fregni, F., 2009. Updates on the use of non-invasive brain stimulation in physical and rehabilitation medicine. *J. Rehabil. Med.* 41, 305–311.
- Wu, A.D., Fregni, F., Simon, D.K., Deblieck, C., Pascual-Leone, A., 2008. Noninvasive brain stimulation for Parkinson's disease and dystonia. *Neurotherapeutics* 5, 345–361.
- Zaghi, S., Acar, M., Hultgren, B., Boggio, P.S., Fregni, F., 2009. Noninvasive brain stimulation with low-intensity electrical currents: putative mechanisms of action for direct and alternating current stimulation. *Neuroscientist* 16, 285–307.
- Zuo, X.N., Di Martino, A., Kelly, C., Shehzad, Z.E., Gee, D.G., Klein, D.F., Castellanos, F.X., Biswal, B.B., Milham, M.P., 2009. The oscillating brain: complex and reliable. *NeuroImage* 49, 1432–1445.